Advancements in the Understanding of Pressure and Temperature Induced Phase Transitions in Solids

Stefano Leoni, Salah Eddine Boulfelfel, Luis Craco, Ulrich Schwarz, and Yuri Grin

Introduction

Finding new pathways to novel materials is a formidable challenge in modern solid state chemistry. One of the reasons which still prevent a rational planning of synthetic routes is the lack of an atomistic understanding at the moment of phase formation. This has motivated a systematic theoretical study of phase transitions [1-6], especially of those processes with first order thermodynamics. This effort is directed to reach a firm understanding of the atomistic mechanisms governing polymorphism in the solid state. In first order phase transitions the new material nucleates within the pristine one, and initially isolated nuclei grow via propagation of phase fronts. Such interfaces may fuse upon domain-domain contacts or turn into grain boundaries resulting in the formation of polycrystalline solids. Understanding the details of such processes entails a rational approach to material synthesis. In general terms, it is the nature of the reactivity in solids that has to be unfolded. Novel theoretical concepts and simulations for direct comparison to the experiments have to be developed. New perspectives emerge from the discovery of the richness of chemical issues beyond the bare thermodynamic classification of phase transitions [6]

Selected Systems

Challenging systems are represented by compound classes, in which many alternative mechanisms can either be suggested on the basis of experimental observations or be derived from crystallographic-geometric approaches. The degree of charge transfer is believed to play a role in selecting a possible intermediate in III-V semiconductors. Nonetheless, there still is an open question whether an intermediate of *h*-BN type structure is relevant for the transformation and how the crossing of a particular intermediate is connected to the transformation mechanism. To clarify this point we used isothermic-isobaric molecular dynamics simulations combined with transition path sampling (TPS). This strategy was developed to tackle the rare event problem connected with activated processes on a large variety of reconstructive phase transitions [1-6]. To study the role of defects on the mechanism we extended the simulation scheme by allowing atomic replacement [3]. The onset of the transition is marked by nucleation and growth of a metastable structure in which the system stays longer than 1 ps. On the other hand, the resolution of time-resolved electronic spectroscopy is around 100 ps and hence, it is only in particular cases helpful in identifying a possible intermediate. A further experimental difficulty is the strong overlap of the tetragonal structure peaks with those of wurtzite and rocksalt in the x-ray powder diffraction (XRD) data refinement. In contrast, the time resolution of our simulations allows for a clear identification of distinct events. The nucleation and growth sequence (wurtzite-tetragonal followed by tetragonal-rocksalt) clearly reflects a two-step transformation mechanism in which the tetragonal intermediate does not simply link the limiting structures in a crystallographic way, but stands as a metastable one, reflecting a different energetic profile of the transition path (Fig. 1).

The *B*4→*B*1 phase transition is observed in other group-13 nitrides like AlN and InN at lower transition pressure. Upon decompression InN and GaN rocksalt phases revert to the wurtzite-type structure. In contrast and as one of a few exceptions in semiconductors, AlN stays in the high-pressure phase down to ambient conditions.

Substitution with indium does not affect the overall transition mechanism and the trajectories stay in the same GaN regime crossing the tetragonal intermediate. The layer shearing direction is maintained while indium exhibits a tendency to form islands where the nucleation preferentially starts. In contrast, aluminium progressively quenches the pathway through the tetragonal intermediate by contrasting phase growth. At 5% cation substitution the tetragonal phase is no longer metastable and phase growth crosses over directly to the rocksalt phase. At this point, the

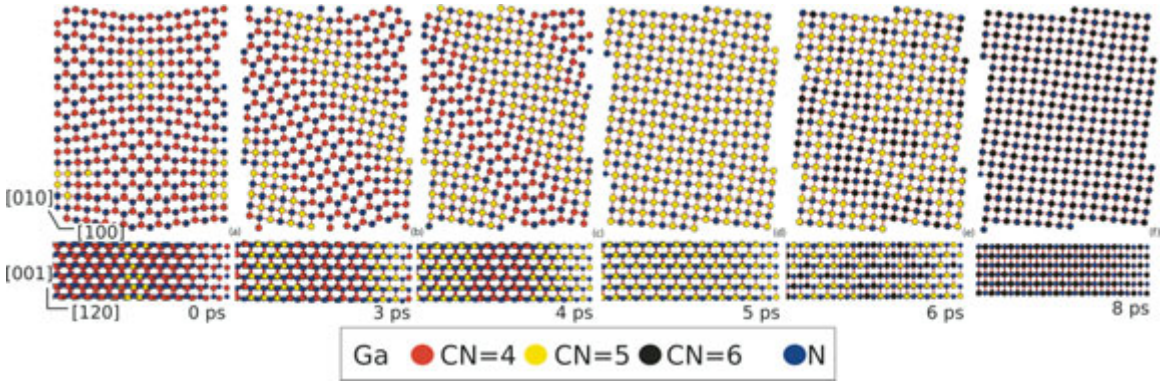

Fig. 1: Snapshots taken from a representative trajectory of the B4→B1 transformation of GaN. The colors reflect the coordination of the Ga atoms. Upper row: (001) plane, lower row: view along [001]. The transition from B4 to B1 crosses an intermediate tetragonal configuration (5 ps) similar to the high-pressure form of tin phosphide, SnP and GeAs

tetragonal structure. survives as an interface between wurtzite-type and rocksalt-type structural motifs. With the removal of the tetragonal intermediate the backward transformation is noticeably modified so that $Al_xGa_{1-x}N$ becomes inert to a transition from *B*1 to *B*4 on further increasing *x*.

The polymorphism of ZnO encompasses three structure types: the wurtzite-like structure *B*4, the zinc-blende metastable variety *B*3, and the high-pressure modification (rocksalt type, *B*1). The wide indirect band gap (2.45 eV) of the cubic phase *B*1 makes it more suitable for high *p*-type doping than the hexagonal variant. Trapping the rocksalt structure at ambient conditions is therefore of great interest [5].

Similar to GaN distinct intermediates can be proposed for the phase transition from B4 to B1. In ZnO, however, a competition between different intermediate structural motifs is apparent from our simulations. The transformation from B4 to B1 occurs with the formation of a tetragonal motif (iT) that characterize the interface between coexisting structural motifs. The *B*4→*B*1 transition in ZnO is accompanied by a large volume collapse (20%). In lower pressure regimes, inside the hysteresis loop, the transformation can branch into a different intermediate (B4→*iH*). While the mechanism leading to B1 over iT involves shearing of layers a compression along *c* prior to the shearing a hexagonal intermediate (iH). The atoms are *quasi*-collectively displaced parallel to $[001]_{B4}$ and the whole system is converted into a hexagonal fivefold intermediate structure. However, as soon as the reconstruction of layers resumes, atoms regain their initial positions within the wurtzite structure under the reversal of the transformation (*iH*→B1, Fig. 2).

Capturing the complex kinetics of structural transformations from theoretical simulations entails working out an atomistic landscape. This allows for a detailed understanding of local structural rearrangements. CdSe is a wide-gap semiconductor which has found extensive use in optical applications for its rich variety of effects in the nanoregime. Under normal conditions, it crystallizes in the wurtzite structure type (B4). Applying moderate pressure (2.5-3.5 GPa) it transforms into the rocksalt structure type (B1).

As a third polymorph, zinc blende (B3 structure type), albeit metastable, does exist. However, the appearance of the material is markedly different from the starting sample due to fragmentation into B3/B4 domains. Our simulations reveal initial nuclei formation in the B1 structure matrix (which

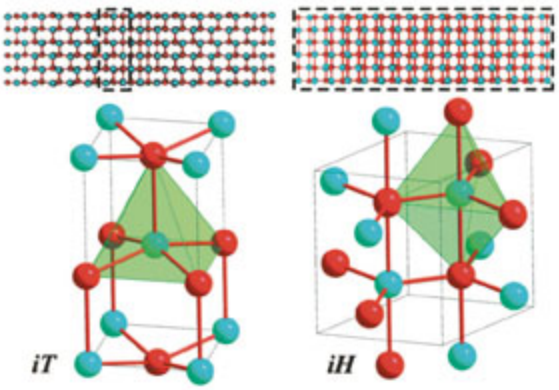

Fig. 2: Intermediate motifs iT and iH. The former is characteristic of the interface between B4 and B1 (upper row, left: inset), along the displacing layers. The latter results from a more collective displacement mode (upper row, right: the whole snapshot shows the same structural motif)

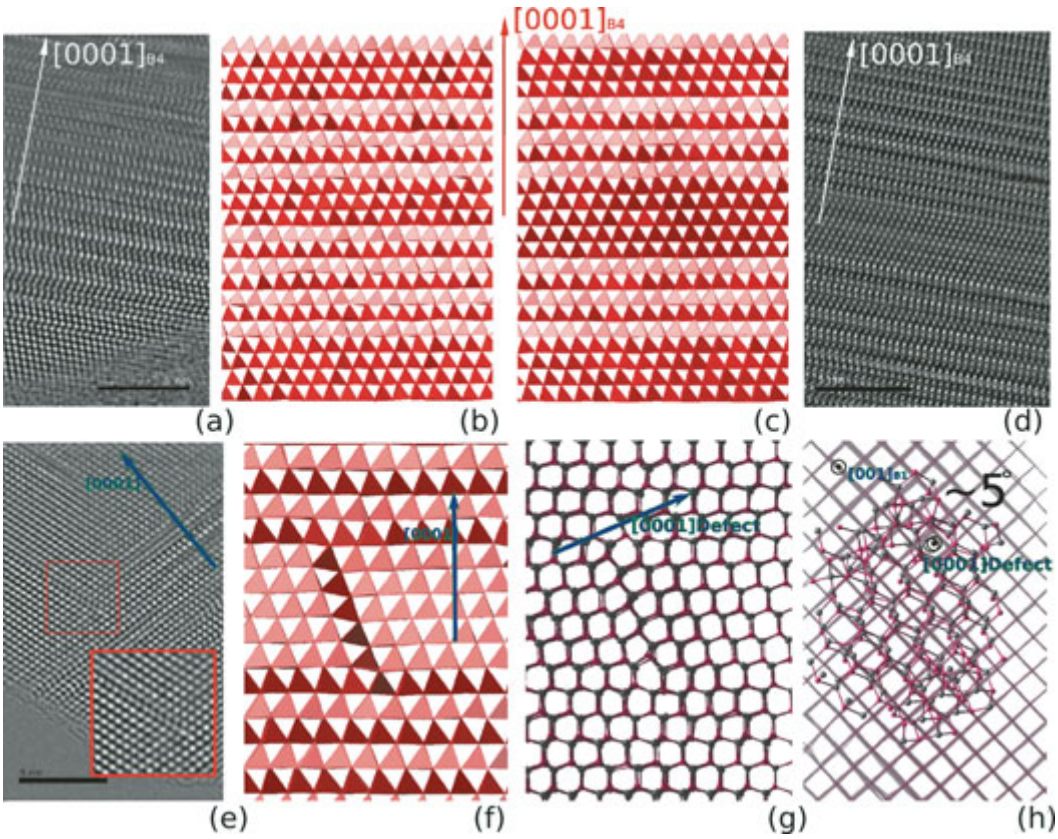

Fig. 3: (Upper row) Lamellar domains of intergrown B3 and B4 motifs. (a and d) HR-TEM images of lamellar domains on pressurized samples. (b and b) Final configuration from MD simulations (P = 3.5-3.8 GPa). (Lower row) Defect formation under pressure and lattice reorientation. (e) HR-TEM image of defects, magnified in the Inset. (f and g) Defects of B4 structural motifs from MD simulations. (h) Alignment of [0001] of the B4 defect with respect to the initial [001] of the B1 structure. An offset of ≈5° is visible.

are of B4 type) followed by regions of B3 structural motifs which grow between already defined B4 regions. The final (sub-) nanodomains result from further growth of this initial configuration. No domain recombination is observed during the growth. Instead, both, B3 and B4, originate from the B1 structure and do not imply intralayer rearrangements. The lamellar final morphology of the material is visible in HR-TEM images (Fig. 3) which exhibit B4 regions with alternating B3 lamellae of different thickness involving 3–5 layers. Due to local rearrangements defects may appear which lead to insets of B4 motifs. The latter separate regions within a B3 domain and terminate inside a B4 domain. These experimental features are precisely identified by our simulations and backtraced to their atomistic generative events [6].

$MgTi_2O_4$ is characterized by a pyrochlore lattice of Ti^{3+} magnetic ions with one single electron in the t_{2g} manifold. It undergoes a very peculiar phase transition from a metallic to a spin singlet insulating phase (MIT) near $T_C = 260$ K. This is accompanied by a structural transition from cubic to tetragonal symmetry with a concomitant drop of the magnetic susceptibility and a resistivity jump at T_C. The structural distortion causes spin dimers to form along shortened Ti-Ti contacts. Our numerical investigations reveal that electronic correlations are fundamental in stabilizing the dimerized ground state of $MgTi_2O_4$ [7]. We show that a MIT is driven by correlation (via LDA+*U*) induced orbital order rearrangement. Therein, *U* controls the band splitting toward an orbital-insulating state *without* full orbital polarization (Fig. 4, upper row). In our picture, orbital order stabilizes the spin-singlet ground state which in turn controls the degree of structural distortions. In the ground-state AFM solution, the canting of the *XZ* orbitals away from the Ti-Ti bond plane becomes significantly smaller when the low-*T* structural distortions are taken into account. Also, the average Ti-O distance in the *XZ* plane (2.068 Å) is appreciably larger than in the *YZ* (2.052 Å) and

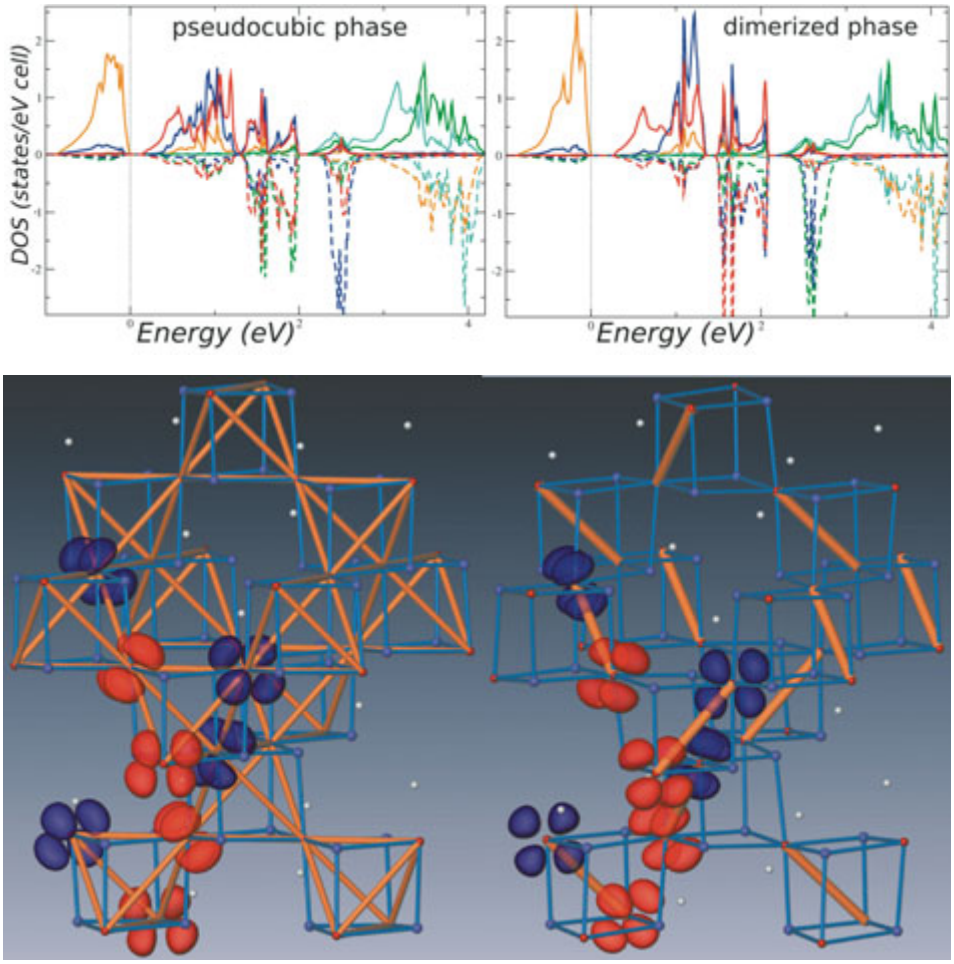

Fig. 4: (Upper row) LSDA+U orbital resolved DOS for U=3 eV in the antiferromagnetic pseudocubic phase (left) and in the antiferromagnetic dimerized phase (right) of $MgTi_2O_4$. Within dimers, DOS of different sites are mirror images with respect to spin space. (Lower row) Orbital ordering of $MgTi_2O_4$ as obtained within LSDA+U, U=3 eV. The red and blue colors denote the ground-state orbital with different (↑,↓) spins.

XY (2.041 Å) planes. Consequently, an occupation of the *XZ* state becomes energetically more favorable. This suggests a novel scenario for quasi-1D chains in the strongly frustrated network of $MgTi_2O_4$ in which the crystal structure itself gets modified by the onset of orbital order (Fig. 4, lower row).

Conclusions

The novel simulation approaches reveal a rich set of chemical effects. Therein, it becomes possible to capture details of phase growth mechanisms with the necessary time resolution. In combination with electronic structure calculations this approach is intended as a powerful tool for materials design and rational synthesis planning.

References

[1] *D. Zahn, S. Leoni,* Phys. Rev. Lett. **92** (2004) 250201.
[2] *S. Boulfelfel, D. Zahn, O. Hochrein, Yu. Grin, and S. Leoni,* Phys. Rev B **74** (2006) 94106.
[3] *S. Boulfelfel, D. Zahn, Yu. Grin, and S. Leoni,* Phys. Rev. Lett. **99** (2007) 125505.
[4] *S. Leoni,* ChemEur J **13** (2007) 10022.
[5] *S. E. Boulfelfel and S. Leoni,* Phys. Rev. B **78** (2008) 125204.
[6] *S. Leoni, R. Ramlau, K. Meier, M. Schmidt, and U. Schwarz,* Proc. Natl. Acad. Sci. **105** (2008) 19612.
[7] *S. Leoni, A. Yaresko, N. Perkins, H. Rosner, L. Craco,* Phys. Rev. B **78** (2008) 5105.